

3D human hands rendering by a six degrees of freedom collaborative robot and a single 2D camera

Michael Boyack¹, Alexandra Sices¹, Bruce Woongyeol Jo²

¹Department of Mechanical Engineering, State University of New York (SUNY), Incheon, Korea

²Advanced Dynamics, Aerospace, and Mechatronic Systems Laboratory, Department of Mechanical Engineering, Tennessee Technological University, Cookeville, United States

Article Info

Article history:

Received Dec 13, 2022

Revised Dec 27, 2022

Accepted Jan 16, 2023

Keywords:

2D camera

3D rendering

Collaborative robot

Human hand

ABSTRACT

Human hands are essential in everyday tasks, mainly manipulating and grasping objects. Thus, accurate and precise three-dimensional (3D) models of digitally reconstructed hands are valuable to the world of ergonomics. A 3D scan-to-render system called the “3D hands model rendering using a 6-degrees of freedom (DoF) collaborative robot” is proposed to ensure that a person receives the best possible outcome for their unique anatomy. The description implies this is using a 6-DoF robot with a two-dimensional (2D) camera sensor that will encompass all forms of the production line in a timely, low-cost, precise, and accurate manner so that an individual can go to and scan their hand and have an actual 3D reconstruction print within the same facility, the same day. It is expected to generate an accurate hand model using structure from motion (SfM) system techniques to create a dense point cloud using photogrammetry. The point cloud is used to develop the tetrahedral mesh of the surface of the hand. This mesh is then refined to filter out the noise of the point cloud. The mesh can produce a precise 3D model that can tailor products to the consumer's needs. The results show the effectiveness of the 3D model of the hand.

This is an open access article under the [CC BY-SA](https://creativecommons.org/licenses/by-sa/4.0/) license.



Corresponding Author:

Bruce Woongyeol Jo

Department of Mechanical Engineering, Tennessee Technological University

Cookeville, TN, United States

Email: b.jo@tntech.edu

1. INTRODUCTION

Human hands are handy and can be considered essential to complete many tasks that humans do daily. Delicate movements and gripping abilities allow for very dexterous skills that have become part of daily life, such as typing on a keyboard or driving a vehicle. Due to this, the development of ergonomics for hand-specific product design has become an essential aspect of the creation process [1], [2]. Ergonomics are used in developing many products, such as work products like gloves and tools, office products like computer keyboards and mice, and recreational products like sports equipment and video game controllers to improve either safety or comfort of the user [3]–[5]. Ergonomics have also been used to develop medical devices to keep the affected area comfortable during the healing period [6]. Hand ergonomics uses hand anthropometry to obtain hand measurements to generate a better, safer, or more comfortable design [7]. As depicted in Figure 1, a biomechanical aspect shows that direct relationship between musculoskeletal injuries and unsuitable hand tools that exacerbate occupational risk factors [8]. Thus, hand ergonomics can be seen not only as providing comfort and aesthetics but as life-saving purposes. Various methods have been employed to obtain such data but overlap in experimental acquisition tended to be the norm when narrowing methodology down to two-dimensional (2D) and three-dimensional (3D) imaging tactics.

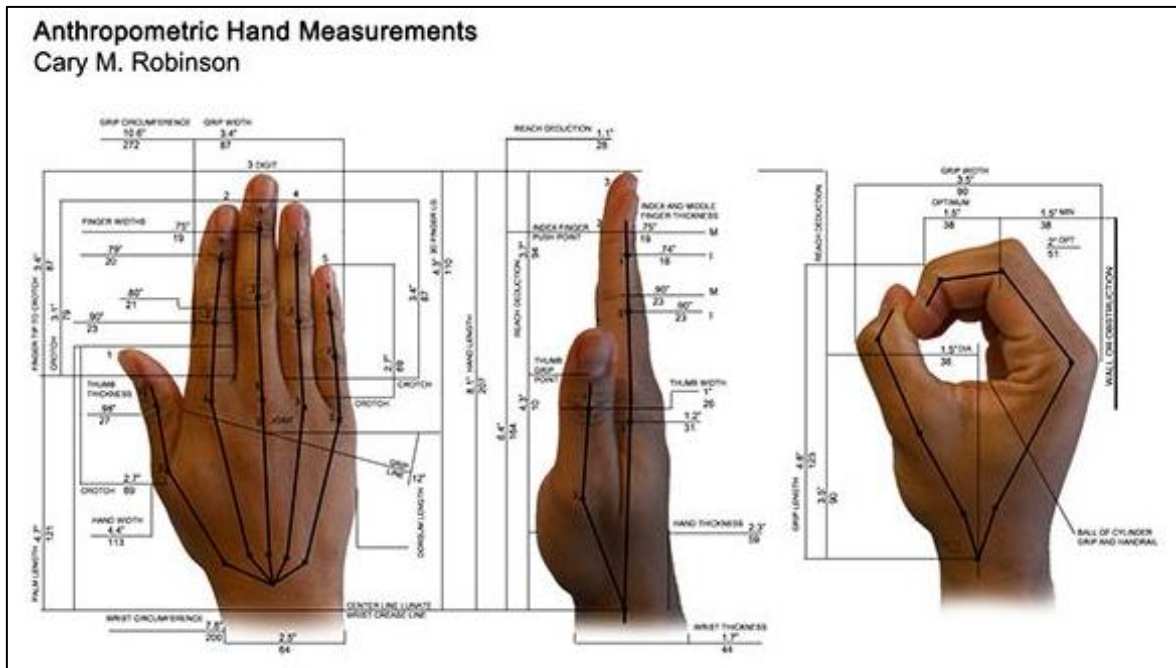


Figure 1. Typical measurements used for ergonomic data for hands

As measuring methods have improved, the anthropometrics used for design have increased, going from a few basic dimensions such as length and width to more complex 2D models that show hand span and finger thickness, to finally, full 3D models of the hand [5]. These measurements are taken using a few techniques. The first is the manual anthropometric acquisition, also known as direct measurement (DM) or direct measurement protocol (DMP), which requires someone to manually take the experimental measurements of the hand. Another technique is 2D image analysis or photogrammetry, where an image is taken of the hand, and then the picture is used to find the dimensions of the hand. The final technique is 3D hand scanning which includes using light detection and ranging (LIDAR) scanners, 3D depth cameras, or multiple images from 2D cameras and critical point clouds to generate a computer model. The 3D scan is important because it is a more precise representation of the hand's complex curvature, which is challenging to model accurately with only manual measurements and which changes from person to person [5], [9].

A few examples of the different types of anthropometric data used in the design and production of objects follow. While designing a wrist brace, Koo and Lee [10] used 3D models of multiple hands to create a brace that mounts better to the shape of a hand. Lee *et al.* [11] described using 3D models of different body parts to evaluate designs of ergonomic military equipment. The reasons that were going for the 3D models include using them in the design and simulation of the product and in the structural analysis of the design. Griffin *et al.* [12] used hand anthropometrics to acquire and overlay multiple hands to develop three specific sizes of gloves so that they fit better as depicted in Figure 2. They also found that due to the lack of hand models on which to base design decisions, many hand-based products need to be better proportioned causing user difficulties.

These studies all took an amalgamation of scans and had difficulty in merging the models together and scaling them correctly. Other difficulties that have occurred during the process of designing objects for human hands relate specifically to the diversity of proportions that occur in human hands. To combat this greater personalization can be used to make products that fit well for one person. The problem with this is the cost of personalized products is much greater than that of mass-produced ones [3]. There are various methods available that can be used to scan a hand. The first option to consider is whether the scan will be done manually, semi-automatically, or fully automatically. Each of these methods has its own advantages and disadvantages [9]. For example, one reference used magnetic resonance imaging (MRI) to create a precise hand model [2], while other articles analyzed their own data acquisition by comparing the hand measurements of a number of participants with varying gender percentages that were taken via direct DM/DMP/manual anthropometry, 2D image analysis or processing/photogrammetry, and 3D imaging. For a manual scan, the scanner system shown in Figure 3 is held by the operator who uses personal judgment to determine the angles and position of the object the scanner views to generate the 3D scan. For this method of

scanning, the advantages are greater flexibility in object size to be scanned, more control over the angle the scanner obtains, and a cheaper price of setup; but the major failings of the system are less accurate repeatability of the scan, longer time to complete a scan, and training is required for the person to operate the scanner [13].



Figure 1. Hand-wearing mal-fitting glove



Figure 2. 3D handheld scanner

For a semi-automatic 3D scanner, the scanner is held by a robotic manipulator and driven by an operator who determines the position and angles used to generate the scan, as shown in Figure 4. This method of scanning has better speed and repeatability than manual scanning but has issues when the size of the object to be scanned is too large. The cost of a semi-automatic scanner is much higher than that of a manual scanner as well [14], [15]. A fully automatic 3D scanner, as in RoboScan [16], has the object placed in a predetermined location and the scanner, which is attached to a robotic manipulator, moves around the object with the position and angles either preset or determined by a program. For the fully automatic method, the advantages are the speed of completing the scan, repeatability of the scan, and accuracy of the scan; the disadvantages are the cost of materials, restrictions to the size of the object scanned, and possible issues with safety. Another decision that must be made for completing 3D scans is what type of scanner will the system use. The three most common systems for 3D scanning are laser rangefinders such as LIDAR, 3D depth cameras such as Microsoft Kinect, and 2D cameras using photogrammetry. Laser range finders are used in [11], [12], [17] to scan the objects and find issues with movement during scanning which can cause defects or distortions in the model. Laser rangefinder scanners are also more expensive and typically take longer to complete a scan.



Figure 3. Stationary scanning system where the object is rotated, and the camera remains still

Yamakazi *et al.* [14] and Pan *et al.* [18] used 2D camera setups due to the inexpensive cost and speed of the scan. However, the computational requirements and processing time are much greater than the laser scanner. The computational cost of the 2D camera is due to the large set of photos that are needed to generate the number of key points to create the point cloud necessary for a 3D model.

The 3D depth camera [19], as shown in Figure 5, is a combination of the laser scanner and the 2D camera as it has a rangefinder attached to a camera that works together to create the model. The computational cost of this method is greater than just the laser rangefinder but less than the 2D camera setup. It is also more resilient to the movement of the object, but the scanning time is longer than the 2D camera setup. To create a full model of an object three different methods are typically used. The first method [20] takes multiple flat models of the object from different angles and merges them together in the correct orientation to generate the final full model. Another method [19] is to have the object held by a gripper attached to the robotic manipulator and rotated in front of the scanner to get the full object model and then remove the gripper from the model. However, this method obtained some small errors in the model due to the pressure from the gripper and the subtraction of the gripping fingers. To use 2D or 3D photogrammetry to

obtain such data in an efficient manner and reconstruct them into 3D object models, a robot manipulator can be used to take photos at many different angles and replace a multi-camera environment for efficiency. One reference used a 6 degree-of-freedom (DoF) robot manipulator with a laser sensor (2D rangefinder) attached to its end-effector and used an iterative-closest point (ICP) algorithm to obtain and then calibrate objects or environments and filtering noise while considering the pose (position and facing angle) of the laser [21]. Here, the laser sensor and 2D camera sensor can be interchangeable, and the same pose considerations can be used. Another usage of 6 DoF robots is in using an RGB-D depth camera such as Microsoft Kinect® connected to a Baxter® robot's manipulator to provide a self-identifying non-collision environment using a 3D point cloud. A simplified 3D model of the robot was generated using the point cloud, and then a collision prediction algorithm was proposed to estimate collision parameters as they would happen in real-time [22].



Figure 4. 3D depth camera

2. PROPOSED METHOD

Based on the points above, it is shown that research has been done to create a good model of the human hand for ergonomic design and medical purposes. However, there are still issues with the current practices used to achieve the model. One issue that occurs is to scan a hand precisely, most of these experiments showed that it was difficult to get a proper scan with an individual's actual hand due to involuntary movement, and thus resorted to creating molds for their data acquisition. Also, the diversity of proportions that occur in human hands makes designing ergonomic devices extremely difficult.

To address these issues our system will scan one person's hands and tailor the product to that person. This personalization will increase the comfort and usability of the product; however, it will also make the product more difficult to manufacture and more costly. These tradeoffs are acceptable because the increase in comfort and usability will make the product more desirable and consumers will pay more for it. For our system to become more fully customizable it must have a method of scanning the hand of the target, modeling the hand, and a method of manufacturing the product.

From the three types of systems discussed above, we decided to go with a fully automatic system for increased speed, accuracy, and repeatability. The increased speed is important because the system will be scanning a live hand and small changes in position could cause issues, and thus a quick scan will minimize mistakes due to those changes in position. Accuracy is also important for the customization that we wish to be able to impart to the product. For our scanning system, we decided to use the 2D camera setup as it is the cheaper option and the scanning (image acquisition) is done at a higher speed and takes less time. The reason this is important is that if the people must hold their hand in one position for a shorter period there will be less movement of the hand and a better model can be made. The main issue of using the 2D camera is the computational cost which is less significant for our application because we need speed during the scan, but the speed is less important once the images have already been acquired. The last method is to use a transparent base to hold the object and use the scanner in all directions of the object.

For our system, we have decided to use the last method and have a transparent base to rest the hand on and have the scanner move around and under this base to get the full model. This will also leave an area around the object where the scanner will not enter which will add to the safety of this scanning method. The complete system consists of a 2D camera attached to a 6 DoF robotic manipulator in an eye-in-hand configuration which creates a 3D model of a human hand which is resting on a transparent base during the scan. This system aims to solve some of the issues that come up with ergonomic design and accessibility. By eliminating the need for a long, arduous process and by getting rid of unwanted contact due to archaic measuring systems, we can provide a more efficient way for people to obtain lifesaving products more quickly.

3. METHOD

The process of creating the 3D scanned model of the hand is complex. However, it can be understood easily if broken up into simpler steps. The procedures are i) hand positioning, ii) 3D scanning commencement, iii) image acquisition, iv) hand removal, v) image processing, vi) point cloud creation, vii) model generation, and viii) model post-processing.

The first and most important is hand positioning. The hand is placed on the transparent barrier with the digits comfortably spaced and the base of the wrist and finger pads being the only part of the hand touching the barrier as depicted in Figure 6. There should not be too much pressure on the hand as that may cause deformation of the hand which is undesirable in the model. The transparent barrier is set to a specific height and held at a set location with regard to the robotic manipulator. The importance of positioning is due to the potential injuries that may occur by the hand being struck by the robotic manipulator.

After the hand has been positioned, the 3D scanning process may be started. The robotic manipulator, which is a Doosan Robotics M1509 model shown in Figure 7 must first be turned on and have the safety limits checked to make sure everything is in order. After that is done, the program is started, and the manipulator moves around the hand in a predetermined path collecting images of the hand from various positions and angles at high speeds. There is a predetermined volume that the manipulator is programmed to avoid which is where the hand must be positioned. The path programming was completed with the built-in system programming language called Doosan Robotic Language (DRL) which is based on Python.

The images are acquired using a Samsung camera which is a camera sensor attached to the Galaxy Note 9 series phone, with 12 megapixels, 1/2.55-inch sensor, dual-pixel PDAF, f/1.5-2.4 variable-aperture lens as shown in Figure 8. This sensor is ideal for our image acquisition because it is both small and light, which means that the manipulator will be able to move at higher speeds. It also can autofocus which should allow a smoother image even if taken while in motion. It can also transmit the images to a laptop over WIFI or Bluetooth. Also attached to the manipulator will be a light to provide good illumination for the hand and to limit images that are unusable due to backlighting. The camera sensor will take many images to be used in the model creation process, along the order of 300 images per model made.

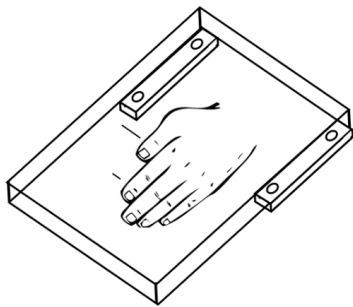


Figure 5. The hand is resting lightly on the transparent barrier in a semi-relaxed manner



Figure 6. Doosan robotics manipulator M1509



Figure 7. Samsung camera which is attached to Galaxy Note 9

After the images are acquired and the robotic manipulator returns to its home position, the hand may be safely removed from atop the transparent barrier. With speed as the focus of the scanning technique, the total time should be five minutes at a maximum in static mode. Once the scanner is finished the images are sent to a computer for processing. The images that are unusable due to poor lighting, reflections from the transparent barrier, blurriness, or other defects will be removed from the data set.

The surviving original images are sent through an open-source program called visual structure from motion (SFM) [23] which creates a model of where the cameras are placed and angled as well as a point cloud of key markers. These key markers are identified using the scale-invariant feature transform (SIFT) method. This method identifies local features in images and identifies a vector that can describe each feature. This set of vectors is used to compare with sets from other images and from those that are close enough to be considered a match across multiple images to create a point that is placed in the point cloud. VisualSFM also sets these points in a 3D space so that the images from the hand can be identified in real space.

The 3D point cloud is made up of many points that will all be on the surface of the hand. By connecting these points in a tetrahedral mesh, the basic model is formed as depicted in Figure 9. The program we will be using creates the mesh by creating a vector between a point and its 8 closest neighbors. If the points overlap with a closer set, then that mesh section is removed from the set of meshes used for the model. After the surface has been suitably modeled it goes through the final processing.

The model processing takes the surface mesh that was created and smooths it out. It removes any jagged edges and lowers peaks so that it models the hand more closely. This is done using a program that computes the derivatives of each mesh line leaving a point and subtly adjusts the point location to minimize

the changes. It will also sort through the point cloud to identify points that are not part of the model and remove those entirely. A series of various views for the data collection process is shown in Figure 10.



Figure 9. 3D point cloud generated from images of a hand

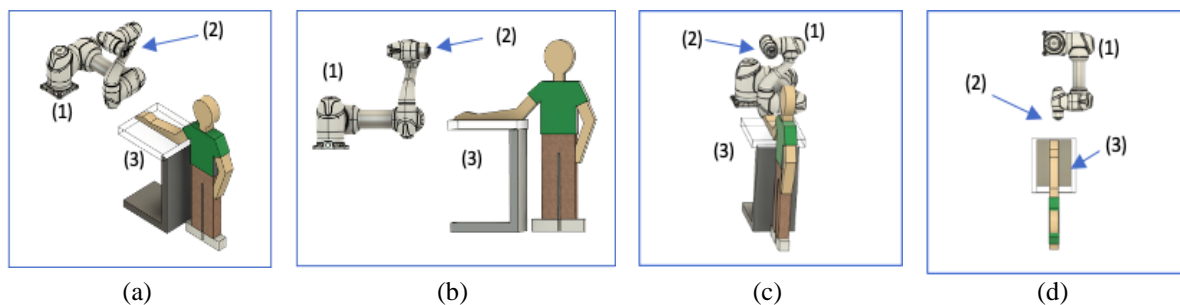


Figure 10. Basic 3D draft of robot manipulator setup and application from (a) a general isometric view, (b) side view, (c) front view, (d) top view, showing the (1) robotic manipulator, (2) 2D camera with a constant light/flash, (3) transparent tray for the hand to stay completely still in rest mode

Through this process, the final model will be created and accurately resemble the hand that has been scanned. This model can then be used for product design, ergonomic studies, or medical research. It can also be used to create a representation of the hand by sending the model to additive manufacturing equipment and printing out a plastic 3D model.

3.1. Hardware

3.1.1 6-DoF robot manipulator: Doosan robotics M1509

The Doosan Robotics M1509, a collaborative robot (a.k.a. cobot) system is intended to directly interact with people in a shared space and/or in proximity. The system consists of a 6 DoF manipulator, as shown in Figure 11, a controller, and a teach pendant, as shown in Figure 12.

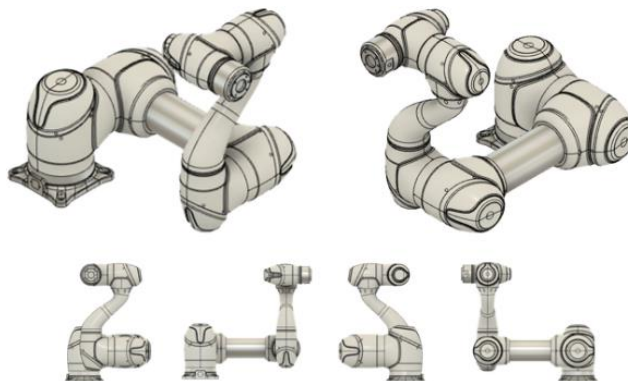


Figure 8. A 3D Model in Autodesk® Fusion 360® with captured isometric views (top), and front, back, and side views (bottom) to show the Doosan Robotics M1509 manipulator in its resting position



Figure 9. The Doosan Robotics M1509's Controller (left), and the Teach Pendant (right)

The manipulator consists of 10 main parts: the base, the links (Link1, Link2), the joints (J1, J2, J3, J4, J5, J6), and the tool flange. The base is grounded to a table while the links act as the appendages of the robot for necessary reach, and the joints rotate to extend and contract the manipulator links as needed. The tool flange is an end-effector located at the tip of the manipulator that allows the installation of sensors and/or other tools, such as grippers, to be attached to it depending on the purpose of the system. While the main system is maintained and regulated through the controller, the manipulator itself has its own backup control system called a cockpit that allows direct teaching and operation [24].

The controller shown in Figure 12 acts as the computer that controls the main functions of the manipulator and its components. It has several input/output (I/O) terminals that connect to the manipulator and teach pendant. It also consists of a power switch, I/O connection terminal, cable connection terminals for both the teach pendant and manipulator, and a power connection terminal for connection to the power supply. The teach pendant, or the device that “teaches” the manipulator how to do its tasks through a programmable interface, consists of a power button with a power LED to indicate when power is on/off, a hand guiding button for more fine-tuned tasks, and an emergency stop button to stop robot operation in case there is an emergency.

3.1.2. 2D camera for sensors

A 2D camera sensor will be attached to the tool flange component of the manipulator and will function as a camera by taking multiple photos of an object (in this case, a hand), and with the help of a microcontroller, its contents will be sent to a point-cloud program to be further processed. A creation that resulted from a collaboration between the Carnegie Mellon Robotics Institute and Charmed Labs, the Pixy2, a CMUcam5 computer vision and control device is a small, cost-friendly, readily available, fast, and easy-to-use vision system with programmable support. It can easily connect to an Arduino or other microcontroller board with the libraries provided and can communicate via a serial peripheral interface (SPI), inter-integrated circuit (I2C), UART, USB, or analog/digital output. It has a configuration utility that runs on various operating systems (OS) such as Windows, MacOS, and Linux, with all software and firmware being GNU-licensed, and supports programming languages such as C++ and Python [15].

3.1.3. Hand rest apparatus

For a hand to remain completely still while the robot manipulator takes the necessary images to create a 3D model, an apparatus can be used as support to ensure that a person's arm can rest comfortably without feeling a need to adjust mid-task. This is done by constructing a table sturdy enough to withstand the weight of a person leaning on it, with one side unobstructed for manipulator movement allowance, and with a hard, transparent material on top that allows a full view of the hand being photographed. A computer assisted design (CAD) imagining of the apparatus is shown in Figure 13, complete with aluminum profile bars, aluminum and steel brackets, and a thick slab of acrylic for the hard, transparent material.

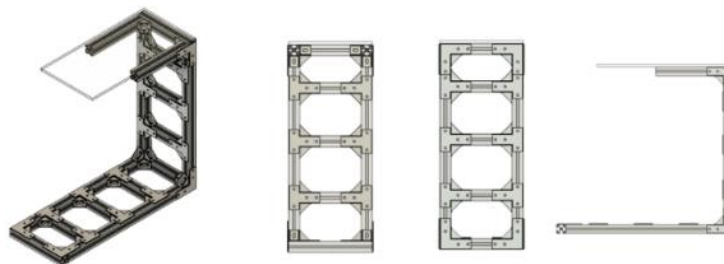


Figure 10. CAD design of the hand rest apparatus in isometric, front, back, and side views

Aluminum profile bars were chosen for the base of the apparatus due to their strength, durability, accessibility, and relatively low cost. Acrylic was used as the hard transparent material for the apparatus top due to low cost, flexibility (as opposed to the brittleness of glass), and out of several transparent materials in the running. It has a refractive index that was closest to air (1.48 and 1.00 [25], respectively) which would mitigate the distortion of the hand. The completed model of the apparatus is shown in Figure 14.



Figure 11. Hand rest apparatus: aluminum profile bars and acrylic slab

3.2. Software

3.2.1 Point-cloud process: VisualSFM system

The photos taken by the 2D camera sensor on the manipulator will need to be processed into a 3D shape, which, in this case, will be done via a point-cloud system. VisualSFM is an open-source photogrammetry software that obtains reliable 2D and 3D data from objects in a real-world environment and creates 3D models from an image or multiple images via 3D dense point clouds. Once the user's environment is set up in a way to VisualSFM command line enables the user to program important features such as the parameters of the model and speed of reconstruction, and then saves all files into node version manager (NVM) files [24]. 3D Rendering and Modeling: Autodesk® Fusion 360®.

Once the photos of the hand are processed into the point-cloud system, it needs to undergo rendering to become a 3D model. If an NVM file from VisualSFM is converted into a stereolithography file, it can be opened in Autodesk® Fusion 360®, a cloud-based platform for Mac and PC for computer-assisted design product development, which has sculpting, modeling, rendering, and generative design tools for a relatively easy-to-use environment. From there the model can be converted via GrabCAD into a coordinate machine binary (CMB) file which can then be sent to the 3D printer to build a prototype of the hand model [26].

3.3 Mathematical model

The point cloud is created by using the SFM process. The process utilized the geometry to create a projection matrix P_i which relates points from 2D image locations (x_i) to a 3D location (X). This can be written as (1).

$$x_i = P_i X \quad (1)$$

Each image needs its own projection matrix because it includes information about the camera's 3D position and orientation, as well as the internal camera parameters such as the focal length, principal point coordinates, aspect ratio, and image skew. Lens distortion is not fixed using this projection matrix and so should be corrected before this step; however, our images were centered on the hand and so the lens distortion was assumed to be negligible for the area of the image that was of most importance to the project.

Given images of a 3D object taken from the left- and right-hand sides, let the respective camera matrices be P_l and P_r and let x_l and x_r be two conjugate points (they are projections of the same 3D object point X from the left and right images). The goal of the intersection is to recover the coordinates of X . The projection equation above for the left image can be rewritten using the cross product as (2).

$$x_l \times P_l X = 0 \quad (2)$$

This is similar to (3).

$$x_r \times P_r X = 0 \quad (3)$$

Since both points correlate to one point (X), they are stacked due to noise. It could be solved via singular value decomposition as shown in Figure 15.

$$\begin{bmatrix} x_l \times P_l \\ x_r \times P_r \end{bmatrix} X = 0 \quad (4)$$

The solution is the null space of the coefficient matrix because the trivial solution where $X = 0$ is not desired. This is solved. This can be generalized for a point in more than two images which improves the accuracy of the point by minimizing the effect of noise. Determining the 3D X locations of the SIFT image points gives us a reliable point cloud that shows the outside surface of the hand.

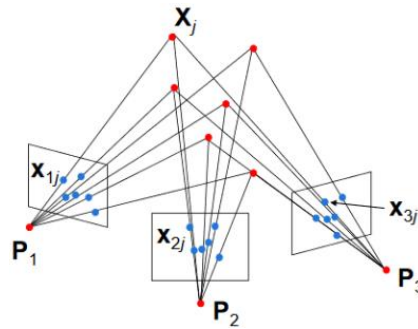


Figure 12. Representation of creating a point cloud based on images from different poses and connecting them to a single global reference frame

4. RESULTS

Using the 6-DoF robotic manipulator and the Samsung camera the following images were acquired as depicted in Figure 16 and processed using VisualSFM. The processed images were then used to create the point cloud of images of the hand. The point cloud was then used as a basis for the model mesh to be created, and the mesh was refined into a solid model.

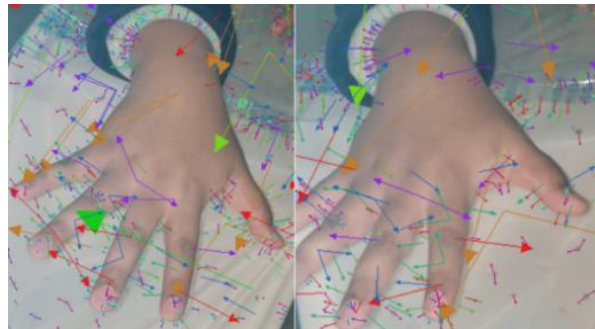


Figure 13. Images of a hand taken using different views: overlaid on the images are the key point vectors which show some similar key points between the two images

Figure 16 shows images of the hand that have had the key point SIFT features overlaid on the image to see the number of key points found. Figure 17 shows the 3D location point cloud generated from these key points that have been matched with more than 3 images from the large data set. Figure 18 shows the camera locations with regard to the hand in the 3D point cloud. As can be seen from the image, while the path of the robot was circular, there are still some noise-based issues from the images. This can be from either the unsteadiness of the movement of the robotic manipulator or also could be due to the blurry images acquired. More filtering of the images could prevent this issue from arising again.

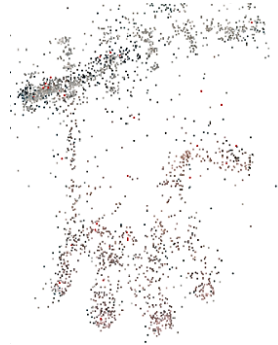


Figure 14. Image of the 3D point cloud created from the SIFT images of the above pictures



Figure 18. Camera locations with regards to the positioning of the hand in three dimensions

Due to the lack of key points created on the dorsal side of the hand, contours were made in different colors to see if they would improve the key point density on the hand. Figure 19 shows the contours that were drawn on the hand to fix this issue. Also, the contours improve the accuracy of the camera locations and eliminate some of the noise caused by the images. We also cut down the number of images used to generate the point cloud due to the increased cloud density. This can be seen from the number of camera locations in Figure 20.



Figure 19. Hand with contours drawn on before scanning



Figure 20. Image of 3D point cloud of contoured hand with camera locations in regard to the positioning

Even with the improved camera locations, there was some noise generated by the movement of the robotic manipulator. Figure 21 depicts a series of images taken of the 3D point cloud that was generated using VisualSFM of the hand used to test the device. The images are from three separate vies so that the point cloud density can be seen to be greatly improved from the previous attempt. The models that are generated are shown in Figure 22. Figure 22(a) is the unrefined base model created by the point cloud. Due to the noise, the surface of the hand is seen to be very coarse and uneven. To make the skin smoother it is processed three times, and the resultant model is shown in Figure 22(b). With the smoothed-out model, the mesh can be exported to an additive manufacturing device or can be used to generate personalized ergonomic equipment.



Figure 15. Point cloud generated from a SIFT Features in 3D from different views

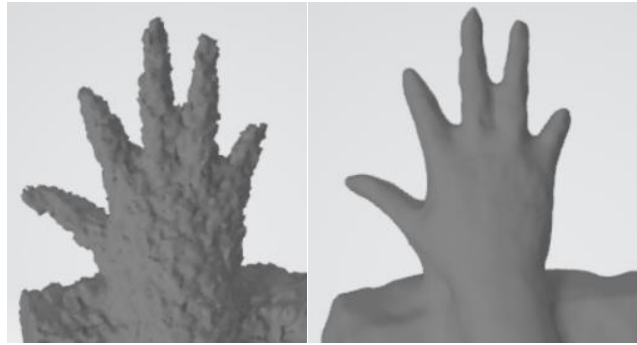


Figure 16. Rendered hand models by 3D point cloud (a) before and (b) after the post-processing

5. CONCLUSION

Based on the previous work, it is possible to generate an accurate model of a human subject's hand using the setup we have proposed. The results show that the point clouds generated from the photogrammetric calculations are sufficiently dense to produce a solid 3D model of the hand. This model can lead to improvements in a personalized ergonomic design which can improve the quality of lives of many people.

Our system still has many improvements to be made. The final model should more precisely reflect the scanned hand to achieve the desired contour for fabricating personalized products. To improve upon this system, future work will include removing background noise from the images prior to processing, filtering the images more precisely, using digital markers such as overlaying a digital skeleton from deep learning to improve locations of the key points, removing some of the glare from the transparent apparatus, improved refining of the 3D model generated.

ACKNOWLEDGEMENTS

We would like to thank Doosan Robotics for providing the 6-DoF robotic manipulator that was essential to this work. This research is supported by the National Research Foundation of Korea (NRF) grant funded by the Korean government (MSIT) (No. 2021R1G1A1012298).




REFERENCES

- [1] J. Marsot and L. Claudon, "Design and ergonomics. methods for integrating ergonomics at hand tool design stage," *International Journal of Occupational Safety and Ergonomics*, vol. 10, no. 1, pp. 13–23, Jan. 2004, doi: 10.1080/10803548.2004.11076591.
- [2] Y. Shimizu, K. Kawaguchi, and S. Kanai, "Constructing MRI-based 3D precise human hand models for product ergonomic assessments," in *Proceedings of Asian Conference on Design and Digital Engineering*, 2010, pp. 837–844.
- [3] A. Zare, A. Choobineh, H. Mokarami, and M. Jahangiri, "The medical gloves assessment tool (MGAT): developing and validating a quantitative tool for assessing the safety and ergonomic features related to medical gloves," *Journal of Nursing Management*, vol. 29, no. 3, pp. 591–601, Apr. 2021, doi: 10.1111/jonm.13188.
- [4] A. Ting and A. Hedge, "An ergonomic evaluation of a hybrid keyboard and game controller," in *Proceedings of the Human Factors and Ergonomics Society Annual Meeting*, Oct. 2001, vol. 45, no. 7, pp. 677–681. doi: 10.1177/154193120104500701.
- [5] A. Yu, K. L. Yick, S. P. Ng, and J. Yip, "2D and 3D anatomical analyses of hand dimensions for custom-made gloves," *Applied Ergonomics*, vol. 44, no. 3, pp. 381–392, May 2013, doi: 10.1016/j.apergo.2012.10.001.
- [6] J. L. Martin, E. Murphy, J. A. Crowe, and B. J. Norris, "Capturing user requirements in medical device development: the role of ergonomics," *Physiological Measurement*, vol. 27, no. 8, pp. 49–62, Aug. 2006, doi: 10.1088/0967-3334/27/8/R01.
- [7] S. K. Kar, S. Ghosh, I. Manna, S. Banerjee, and P. Dhara, "An investigation of hand anthropometry of agricultural workers," *Journal of Human Ecology*, vol. 14, no. 1, pp. 57–62, Jan. 2003, doi: 10.1080/09709274.2003.11905598.
- [8] E. Habibi, S. Soury, and A. Zadeh, "Precise evaluation of anthropometric 2D software processing of hand in comparison with direct method," *Journal of Medical Signals and Sensors*, vol. 3, no. 4, 2013, doi: 10.4103/2228-7477.128338.
- [9] W. Lee, S. Yoon, and H. You, "Development of a 3D semi-automatic measurement protocol for hand anthropometric measurement," *Proceedings of the Human Factors and Ergonomics Society Annual Meeting*, vol. 54, no. 20, pp. 1780–1784, Sep. 2010, doi: 10.1177/154193121005402008.
- [10] D. S. Koo and J. R. Lee, "The development of a wrist brace using 3D scanner and 3D printer," *Fashion and Textile Research Journal*, vol. 19, no. 3, pp. 312–319, Jun. 2017, doi: 10.5805/SFTI.2017.19.3.312.
- [11] W. Lee *et al.*, "3D scan to product design: methods, techniques, and cases," in *Proceedings of the 6th International Conference on 3D Body Scanning Technologies, Lugano, Switzerland*, Oct. 2015, pp. 168–174. doi: 10.15221/15.168.
- [12] L. Griffin, S. Sokolowski, and E. Seifert, "Process considerations in 3D hand anthropometric data collection," in *Proceedings of 3DBODY.TECH 2018 - 9th International Conference and Exhibition on 3D Body Scanning and Processing Technologies, Lugano, Switzerland, 16-17 Oct. 2018*, Oct. 2018, pp. 123–123. doi: 10.15221/18.123.
- [13] B. Sheng, F. Zhao, X. Yin, C. Zhang, H. Wang, and P. Huang, "A lightweight surface reconstruction method for online 3D scanning point cloud data oriented toward 3D printing," *Mathematical Problems in Engineering*, vol. 2018, pp. 1–16, 2018, doi: 10.1155/2018/4673849.
- [14] K. Yamazaki, M. Tomono, T. Tsubouchi, and S. Yuta, "3-D object modeling by a camera equipped on a mobile robot," in *IEEE*




- International Conference on Robotics and Automation*, 2004, vol. 2004, no. 2, pp. 1399–1405. doi: 10.1109/ROBOT.2004.1308020.
- [15] L. Torabi and K. Gupta, “An autonomous six-DoF eye-in-hand system for in situ 3D object modeling,” *The International Journal of Robotics Research*, vol. 31, no. 1, pp. 82–100, Jan. 2012, doi: 10.1177/0278364911425836.
- [16] M. Callieri *et al.*, “RoboScan: an automatic system for accurate and unattended 3D scanning,” in *Proceedings 2nd International Symposium on 3D Data Processing, Visualization and Transmission*, 2004, pp. 805–812. doi: 10.1109/TDPVT.2004.1335398.
- [17] J. I. Vasquez-Gomez, L. E. Sucar, and R. Murrieta-Cid, “View planning for 3D object reconstruction with a mobile manipulator robot,” in *2014 IEEE/RSJ International Conference on Intelligent Robots and Systems*, Sep. 2014, pp. 4227–4233. doi: 10.1109/IROS.2014.6943158.
- [18] Q. Pan, G. Reitmayr, and T. Drummond, “ProFORMA: Probabilistic feature-based on-line rapid model acquisition,” in *Proceedings of the British Machine Vision Conference 2009*, 2009, pp. 112.1–112.11. doi: 10.5244/C.23.112.
- [19] M. Krainin, B. Curless, and D. Fox, “Autonomous generation of complete 3D object models using next best view manipulation planning,” in *2011 IEEE International Conference on Robotics and Automation*, May 2011, pp. 5031–5037. doi: 10.1109/ICRA.2011.5980429.
- [20] L.-C. Chen, D.-C. Hoang, T.-T. Chu, and H.-I. Lin, “Development of registration methodology to 3-D point clouds in robot scanning,” *MATEC Web of Conferences*, vol. 71, Aug. 2016, doi: 10.1051/mateconf/20167104008.
- [21] A. Peters, A. Schmidt, and A. C. Knoll, “Extrinsic calibration of an eye-in-hand 2D LiDAR sensor in unstructured environments using ICP,” *IEEE Robotics and Automation Letters*, vol. 5, no. 2, pp. 929–936, Apr. 2020, doi: 10.1109/LRA.2020.2965878.
- [22] X. Wang, C. Yang, Z. Ju, H. Ma, and M. Fu, “Robot manipulator self-identification for surrounding obstacle detection,” *Multimedia Tools and Applications*, vol. 76, no. 5, pp. 6495–6520, Mar. 2017, doi: 10.1007/s11042-016-3275-8.
- [23] C. Wu, “VisualSFM: A visual structure from motion system,” 2011.
- [24] D.R. Inc., “Doosan robotics installation manual V2.7.1 v2.1 EN.” Republic of Korea, 2020.
- [25] “Refractive index common liquids, solids and gases,” *The Engineering ToolBox*, 2008. https://www.engineeringtoolbox.com/refractive-index-d_1264.html (accessed Apr. 25, 2022).
- [26] “Getting started with fusion 360,” *Fusion 360*, 2021. <https://help.autodesk.com/view/fusion360/ENU/?guid=GUID-1C665B4D-7BF7-4FDF-98B0-AA7EE12B5AC2> (accessed Apr. 20, 2022).

BIOGRAPHIES OF AUTHORS






Michael Boyack    is a Ph.D. student in the Department of Mechanical Engineering at The State University of New York (SUNY), Korea. He can be contacted at Michael.boyack@sunykorea.ac.kr.



Alexandra Sices    is currently an M.S. student in the Department of Mechanical Engineering at The State University of New York (SUNY), Korea. She completed her Associate of Science degree in Mechanical Engineering from Montgomery College, MD, and then earned her Bachelor of Engineering degree in Mechanical Engineering from Stony Brook University, NY in December 2021. He can be contacted at Alexandra.sices@sunykorea.ac.kr.



Bruce Woongyeol Jo    is an associate professor in the Department of Mechanical Engineering at Tennessee Technological University, Cookeville, TN USA. Before, he was an associate professor at the State University of New York (SUNY) Stony Brook, and a tenured associate professor at Tennessee State University (TSU), Nashville TN. Prior to that, he also worked as a tenure-track assistant professor at Embry-Riddle Aeronautical University during 2011-2014 and at Florida State University as a research associate during 2010-2011. His main research interests are i) the design and control of morphorous structures (4D printing), ii) the design of flight control systems, iii) the dynamics/kinematics and mechanism design of mechanical systems, and iv) the design of feedback control allocator for manned/unmanned aerial vehicles in the applications of aerospace, mechanical, and robotic systems. Since 2016, he has been working for and collaborating with many government agencies in the United States including the Air Force Office of Scientific Research (AFOSR), Air Force Research Laboratory (AFRL), ARL (ARL), and Oak Ridge National Laboratory (ORNL). He earned his Ph.D. in mechanical engineering from Columbia University, NY in 2010, his M.S. in mechanical engineering from New York University, NY in 2006, and his B.S. in Electrical Engineering in 2003. He can be contacted at b.jo@tntech.edu.